

# Preparation of Hydrogen-rich Gas by Catalytic Pyrolysis of Straw-plastic Mixture with Nickel-based Honeycomb Cinder

Zeshan Li, Yiran Zhang, Tao Xiong, Bolin Li, Menghan Xiao, Xianzhou Xu, Rui Hu, Yuan Zhu, and Jianfen Li \*

Nickel catalyst supported on honeycomb cinder (Ni/HC) was prepared by a homogeneous precipitation method. The catalyst was applied to produce hydrogen-rich combustible gas by catalytic pyrolysis of soybean straw and plastic (PE) mixture. The straw and plastic materials were analyzed by elemental analysis and industrial analysis. The support and catalyst were characterized by X-ray fluorescence (XRF), X-ray diffraction (XRD), scanning electron microscopy (SEM), and N<sub>2</sub> adsorption-desorption isotherm (BET). The analysis showed that NiO was well loaded on the surface of honeycomb coal slag carrier. The effects of Ni loading, pyrolysis temperature, holding time, and calcination temperature on the experimental results were studied. The results showed that the preparation of the catalyst was feasible and that it had a good catalytic effect. When Ni loading was 15 wt.%, catalytic pyrolysis temperature was 700 °C, holding time was 20 min, and calcination temperature of catalyst was 400 °C, H<sub>2</sub> concentration increased from 20.6 to 52.8 vol.%, and while H<sub>2</sub> yield was 302 mL/g, CH<sub>4</sub> concentration decreased from 51.1 to 22.6 Vol.% and CO concentration increased from 10.8 to 17.8 vol.%. After the catalyst was regenerated 6 times, the H<sub>2</sub> concentration still reached 40 vol.% and the combustible gas concentration was still above 80 vol.%. The catalyst still had good catalytic activity.

*Keywords:* Ni/HC; Catalytic pyrolysis; Soybean straw; Plastic (PE); Combustible gas

*Contact information:* School of Chemical and Environmental Engineering, Wuhan Polytechnic University, Wuhan 430023 China; \*Corresponding author: lijfen@163.com

## INTRODUCTION

With the continuous development of socioeconomic and environmental problems related to the growth of energy consumption led by fossil energy, it is necessary to seek a new sustainable energy source to replace fossil fuels (Saxena *et al.* 2009). Biomass is a renewable raw material, which can consist of straw and other materials. It can be converted into solid, liquid, and gas fuels by chemical or biological processes. Pyrolysis of biomass straw to produce combustible gas has been widely studied (Fahmy *et al.* 2018). However, due to the high oxygen content of biomass, the H<sub>2</sub> content produced by biomass straw pyrolysis is low, and the tar content is high, and there is a need for some method to reduce the tar content (Anis and Zainal 2011). In addition, because the availability of biomass waste varies with seasons, other materials (such as waste plastics) are needed to maintain a stable raw material supply during a given biomass off-season period (Alvarez *et al.* 2014).

With the rapid development of urbanization and industrialization, the demand for plastics is increasing daily. Plastic waste has gradually become the main problem in the global waste treatment. In many countries, landfilling is still the preferred way to treat

waste plastics (Block *et al.* 2018). Landfill treatment of plastic waste will cause serious air, water, and soil pollution, so more effective and environmentally friendly methods are needed.

The degradation of plastic waste by pyrolysis is one of the most environmentally friendly and sustainable methods (Chen *et al.* 2015). During the pyrolysis/gasification process, plastics can be decomposed for H<sub>2</sub> production within minutes at high efficiency (Chai *et al.* 2020). However, plastics are easily melted and stuck on the surface of reactor tubes to restrict continuous feed of fresh plastic (Block *et al.* 2018). Therefore, low or even zero oxygen content materials (such as waste plastics) can be co-pyrolyzed with straw. Among the waste plastics, polyethylene (PE) formed by olefin polymerization accounts for 40% of the total waste plastics, which can be used as raw material for biomass co-pyrolysis (Miskolczi *et al.* 2004). Some studies have shown that in the steam gasification process, increasing the proportion of plastic in the biomass plastic feed will increase the conversion rate of fuel to natural gas and reduce the production of charcoal and tar (Moghadam *et al.* 2014; Lopez *et al.* 2015). In addition, compared to pyrolysis/gasification of only plastics or biomass, higher H<sub>2</sub> production and lower tar/char yields are realized because the high H/C ratio of plastics can compensate for the high oxygen composition of biomass (Block *et al.* 2018). Hence, the co-feeding of lignocellulose with waste plastics in catalytic pyrolysis is beneficial for the environment and energy recapture (Zhang *et al.* 2016).

Catalytic pyrolysis of biomass has been the focus of many researchers in recent years (Ahrenfeldt *et al.* 2013; Wang *et al.* 2017; Fahmy *et al.* 2018), and the treatment of solid waste is also regarded as a major problem facing the world, especially waste plastics, which are difficult to degrade (Zhou *et al.* 2014). Hydrogen production from plastics *via* pyrolysis is desirable, but more carbon is deposited on the catalyst surface than in biomass pyrolysis (Yao *et al.* 2017; Xu *et al.* 2020). Other researchers have conducted co-pyrolysis of biomass and plastic waste from the perspective of co-pyrolysis, but most of them are based on the research and synergy of co-pyrolysis/gasification to produce bio-oil (Levine and Broadbelt 2009; Zhang *et al.* 2014; Burra and Gupta 2018; Ghorbannezhad *et al.* 2020). There have been relatively few studies on gas products, especially the preparation of hydrogen-rich combustible gas. Among catalytic pyrolysis studies, there has been attention to the use of gasifiers to purify gas products. The use of catalysts and gasifiers can improve the gas production in co-pyrolysis, especially the increase of H<sub>2</sub>. Chai *et al.* (2020) used a Ni-CaO-C catalyst in the co-gasification experiment of biomass and plastics (mixing ratio of 5:5), which can achieve high H<sub>2</sub> production (86.7 mol% and 115.3 mmol/g) and low CO<sub>2</sub> concentration (7.3 mol%). Deparros *et al.* (2019) studied the co-pyrolysis and CO<sub>2</sub> gasification of paper polystyrene blends at different mixing ratios using a laboratory scale tubular reactor and thermogravimetric analysis. It was found that co-pyrolysis had a positive effect on the yield of syngas and had a synergistic effect on cracking reaction, resulting in an increase in gas yield and a nearly doubling of hydrogen yield. Co-gasification with CO<sub>2</sub> can improve the co-conversion rate and the total gas yield. Cao *et al.* (2019) studied the combined gasification of biomass and municipal solid waste in a fluidized bed gasifier. When the mixing ratio increased from 100% SD (sawdust) to 100% MSW (municipal solid waste), the volume fractions of CO and CH<sub>4</sub> ranged from 16.7 vol% to 18.8 vol% and from 4.1 vol% to 5.1 vol%, respectively, while the variation trends of H<sub>2</sub> and CO<sub>2</sub> were opposite. Xu *et al.* (2020) used a Ni/ $\gamma$ -Al<sub>2</sub>O<sub>3</sub> catalyst to co-gasify biomass and waste plastics to produce syngas. The results showed that when PE was blended with RH, especially when PE content was 50%, there was a synergistic effect on gas yield and tar yield. For higher PE content (> 50%), the reduction of total gas and H<sub>2</sub> is due to the fact

that chain hydrocarbons with relatively large molecular sizes produced by more PE volatiles are more difficult to crack than oxygen-containing compounds produced by RH volatiles.

The use of a catalyst can improve the content of combustible gas produced by co-pyrolysis of biomass and plastics, especially the content of hydrogen (Grams and Ruppert 2017). In the use of many catalysts, Al<sub>2</sub>O<sub>3</sub> is widely used as a carrier (Zhang *et al.* 2018), because of its high specific surface area to provide suitable Ni dispersion and its mechanical strength that ensures the stability of the catalyst (Charisiou *et al.* 2017). Unfortunately, a large number of acid sites on the surface of alumina promote coke formation and rapid deactivation of Ni/Al<sub>2</sub>O<sub>3</sub> catalysts (Chen *et al.* 2019). In addition, some solid wastes can be used as catalyst carriers. Lan *et al.* (2019) prepared an Ni/FA catalyst with fly ash as support for catalytic pyrolysis of rice straw. When nickel loading was 20 wt.%, H<sub>2</sub> concentration could be increased from 7 vol.% to 41 vol.% at 600 °C. Honeycomb coal (HC) is commonly used in rural heating furnaces in northern China. Its honeycomb structure is conducive to full combustion. Most of the coal cinder waste after combustion is directly stacked and transported, and a small proportion has been used for the potting of plants. The honeycomb cinder contains oxides such as SiO<sub>2</sub> and Al<sub>2</sub>O<sub>3</sub>, which can be used as catalyst support. However, there have been few studies on it.

In this paper, with honeycomb cinder (HC) as the support of nickel-based catalyst, an Ni/HC catalyst was prepared by the deposition precipitation method, which was used for the co-catalytic pyrolysis of soybean straw and polyethylene (PE) to produce combustible gas. The influence of co-pyrolysis parameters on the content of combustible gas was considered.

## EXPERIMENTAL

### Materials

Soybean straw (SS), which was collected in Lvliang, Shanxi Province, China, was chosen as the biomass feed stock. Polyethylene powder (PE: 40 mesh) was used as an ideal substitute for waste plastics. Prior to testing, the soybean straw was crushed and sieved to obtain particles that were size 60-mesh and lower. The two kinds of raw materials were dried at 105 °C for 24 h and then sealed for storage. The ultimate and proximate analysis of the soybean straw and PE samples (Table 1) were conducted using an elemental analyzer (Flash 2000, Thermo Fisher Scientific, Waltham, MA, USA), according to GB/T standard 28731 (2012). Honeycomb cinder was taken from Lvliang, Shanxi Province, China.

**Table 1.** Proximate and Ultimate Analyses of the Soybean Straw and PE

Materials	Ultimate Analysis (wt.%)					Proximate Analysis (wt.%)			
	C	H	O*	N	S	M	A	V	FC
Soybean Straw	41.08	5.53	52.13	1.26	0	4.6	8.7	82.06	4.64
PE	85.78	14.22	-	-	-		<0.05	99.95	

\* by difference; M: Moisture; V: Volatile matter; A: Ash; FC: Fixed Carbon

### Preparation of catalyst

The honeycomb cinder (HC) was crushed and screened to 60-mesh, sealed, and stored. Ni/HC catalyst was prepared *via* the homogeneous precipitation method with  $\text{Ni}(\text{NO}_3)_2 \cdot 6\text{H}_2\text{O}$  as the nickel precursor and HC as the support. First, 5 g of HC was placed in a 500 mL three neck flask, and then  $\text{Ni}(\text{NO}_3)_2 \cdot 6\text{H}_2\text{O}$  and  $\text{CON}_2\text{H}_4$  (in a mass ratio of 1:4) were mixed with 100 mL of deionized water.

After the mixture was completely dissolved, it was poured into a three-neck flask, stirred in an oil bath at 115 °C for 2 h, and aged for 6 h. Next, the mixture was filtered and washed. It was dried at 105 °C for 12 h. The dried catalyst precursor was calcined in a muffle furnace at a set temperature for 2 h to obtain the catalyst (NiO/HC). The catalysts were prepared with different parameters, as follows: a Ni loading amount of 5 wt%, 10 wt%, 15 wt%, and 20 wt% and a calcination temperature of 400 °C, 500 °C, 600 °C, 700 °C, and 800 °C.

### Instruments and Experimental Methods

The experimental device is shown in Fig. 1, which included a gas supply system, pyrolysis reactor, gas purification device, gas collection bag, and analysis system. The tests were conducted in a horizontal fixed-bed quartz tube reactor. The furnace was on the top of the tube reactor and surrounded the quartz tube to ensure that it was heated. Two quartz boats were each used to separately hold the materials and catalyst, with an inner diameter of 40 mm, a length of 100 mm, and a height of 10 mm.

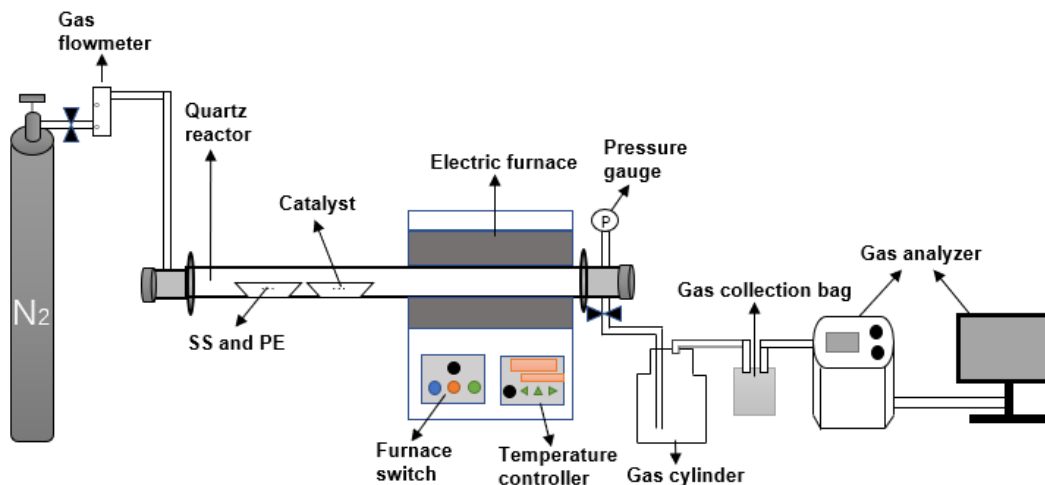


**Fig. 1.** Schematic diagram of the experimental system

The reactor had an inner diameter of approximately 60 mm, a total length of 1400 mm, and a flat-temperature zone of 600 mm. The gas purification device was placed in an ice water bath to completely eliminate the influence of tar.

First, 2 g of straw plastic mixture (the ratio of straw to plastic was 1:1), and 1 g of catalyst were put into two quartz boats in the reactor, and then the flanges on both sides were closed. Nitrogen at a flow rate of 500 mL/min was continuously introduced into the entire system for 30 min under room temperature to ensure an oxygen-free environment. Subsequently, the reactor temperature was increased from room temperature to the specified temperature (500, 600, 700, and 800 °C,) at a heating rate of 10 °C/min and maintained for a specified time (5 min to 30 min). When the flat-temperature zone was preheated to the target temperature, the two boats were quickly pushed into the furnace.

After the reaction time reached the set time, the furnace was pushed away and the valves on both sides of the tube were opened. Meanwhile, the gas was collected in the gas sample bag. Finally, the gas composition and content of the syngas were determined via the gas analyzer. Each group of tests was repeated three times to take the average value and to ensure the reliability of the collected data.

## Methods

The elemental composition and material structure of the catalysts were analyzed via X-ray fluorescence spectrometry (EDX-7000, Shimadzu, Kyoto, Japan) and X-ray diffraction (XRD-7000, Shimadzu). The specific surface area and pore structure of the support, catalyst, and used catalyst were measured via a surface area analyzer (ASAP 2460, Micromeritics, Atlanta, GA, USA). The microstructure of the support, catalyst, and used catalyst were analyzed via scanning electron microscopy (JSM-7100F, Jeol, Tokyo, Japan). The gas product was collected with a gas sample bag and analyzed using an infrared gas analyzer (Gasboard-3100, Cubic-Ruiyi, Wuhan, China).

## RESULTS AND DISCUSSION

### Characterization of the Ni/HC Catalyst

#### *X-ray fluorescence analysis*

The elemental compositions of the HC and Ni/HC catalysts are shown in Table 2. The XRF spectrum showed high contents of SiO<sub>2</sub> and Al<sub>2</sub>O<sub>3</sub> in the Ni/HC catalyst. Different species of alkali metal oxides (*e.g.*, CaO, K<sub>2</sub>O, and TiO<sub>2</sub>) and transition metal oxides (*e.g.*, Fe<sub>2</sub>O<sub>3</sub>) were also detected, indicating that Ni/HC consisted of diverse chemical components. The content of NiO in the Ni/HC catalyst was 22.5 wt.%, which was higher than the theoretical loading of 19.07% (Ni loading 15%). This may have been because XRF analysis is mainly used for the micro-areas of the catalyst surface and is considered a semi-quantitative analysis (Bo *et al.* 2008), which may have led to some errors.

**Table 2.** XRF Analyses of the Honeycomb (HC) Cinder and Ni/HC Catalyst

Sample	Main Composition and Content (wt.%)							
	NiO	SiO <sub>2</sub>	Al <sub>2</sub> O <sub>3</sub>	Fe <sub>2</sub> O <sub>3</sub>	CaO	K <sub>2</sub> O	TiO <sub>2</sub>	SO <sub>3</sub>
HC	-	61.42	25.42	5.42	3.35	2.19	1.02	0.85
NiO/HC	22.54	48.76	15.59	5.23	2.62	2.01	0.95	0.7

#### *X-ray diffraction (XRD) analysis*

Figure 2 shows the XRD spectra of the HC and Ni/HC catalysts. There were characteristic peaks at  $2\theta$  values of 20.7°, 26.5°, 41.6°, and 59.9° that corresponded to quartz (SiO<sub>2</sub>). The characteristic peaks at  $2\theta$  values of 26.5°, 35.1°, and 68° corresponded to Al<sub>2</sub>O<sub>3</sub>. Furthermore, the crystalline phases at  $2\theta$  values of 33.2°, 39.3°, and 49.8° corresponded to Fe<sub>2</sub>O<sub>3</sub>. The Ni/HC catalysts exhibited four distinguished peaks from  $2\theta$  values of 36° to 80° that indicate the presence of NiO. Therefore, it was concluded that Ni was present in the form of NiO, which coincided with the XRF analysis. The peaks at 44.5°, 51.8°, and 76° were identified as the characteristic peaks of Ni, and the active component changed from NiO to elemental Ni.

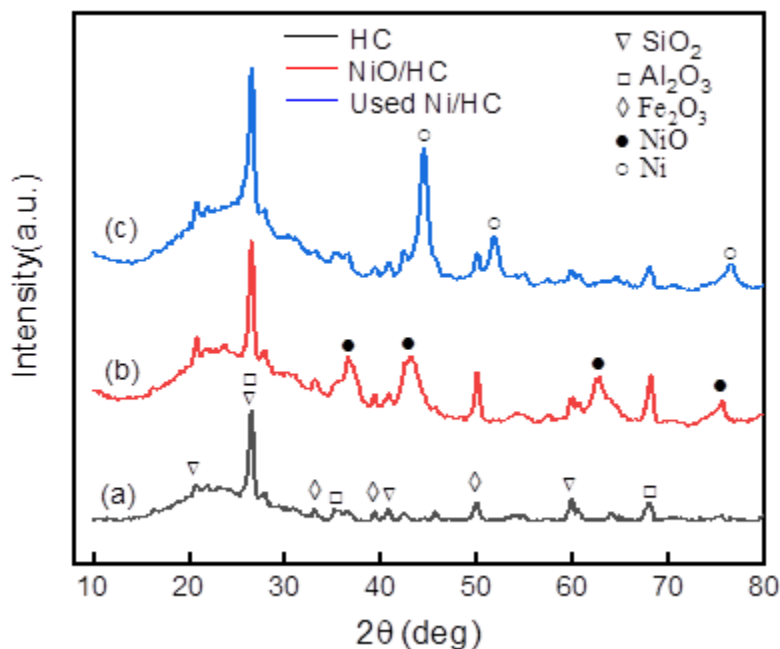


**Fig. 2.** XRD patterns of HC and Ni/HC catalysts

#### Scanning electron microscope (SEM) analysis

The surface morphology of the HC and Ni/HC catalyst are presented in Fig. 3. Figure 3(a) shows that HC consists of lumps of different sizes. Figure 3(b) shows that NiO was uniformly loaded on the support HC, and the structure of the catalyst was relatively complete, which is conducive to improving the activity of the catalyst. Figure 3(c) shows that the surface of HC was covered by deposited carbon, and most of the deposited carbon was filamentous carbon.

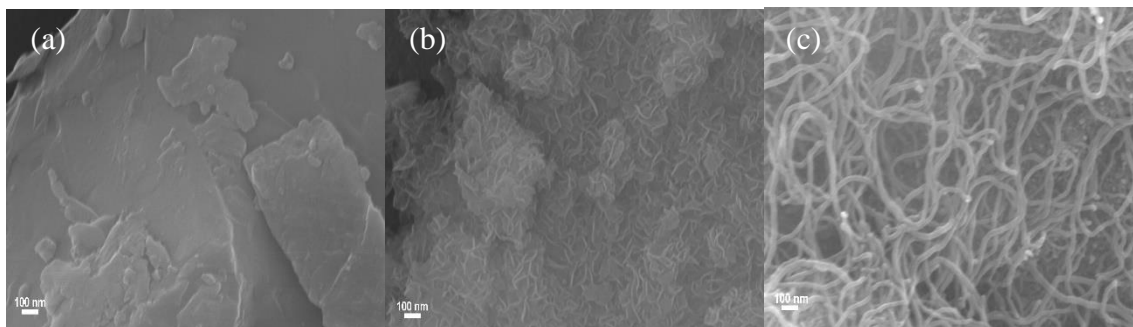


**Fig. 3.** SEM images of (a) HC, (b) Ni/HC, (c) used Ni/HC

#### Brunauer–Emmett–Taylor (BET) analysis

The textural properties of the carrier, fresh catalyst, and used catalyst are listed in Table 3. According to Table 3, the BET surface area of the fresh catalyst ( $26.5 \text{ m}^2 \cdot \text{g}^{-1}$ ) was much larger than that of the carrier, which was  $0.78 \text{ m}^2 \cdot \text{g}^{-1}$ . This is due to the network structure formed by the loading of Ni (Fig 3b), which leads to an increase in the specific surface area of the catalyst. A higher BET surface area of the catalyst meant that there were more active sites on the surface for the catalytic pyrolysis reaction to occur. In addition,

the total pore volume increased from 0.0027 to 0.0875 cm<sup>3</sup>•g<sup>-1</sup>. Furthermore, after the catalytic pyrolysis reaction, the BET surface area and total pore volume of Ni/HC increased and the average pore diameter decreased, mainly due to more coke deposition on the catalyst. There were large amounts of filamentous coke and amorphous carbon on the catalyst surface due to the presence of PE, and some filamentous carbon are known to be carbon nanotubes (Xu *et al.* 2020). This result is consistent with the observation in Fig. 3(c).

**Table 3.** Textural Properties of Carrier, Fresh, and Used Catalyst

Textural Properties	HC	Fresh Ni/HC	Used Ni/HC
BET surface area (m <sup>2</sup> •g <sup>-1</sup> )	0.78	26.49	66.65
Total pore volume (cm <sup>3</sup> •g <sup>-1</sup> )	0.0027	0.0875	0.1319
Average pore diameter (nm)	21.78	13.01	9.49

### Application of Ni/HC catalyst in co-pyrolysis of straw plastic mixture

When the proportion of plastic in the mixture is more than 50%, the hydrogen content produced by pyrolysis will decrease (Chai *et al.* 2020; Xu *et al.* 2020). Therefore, the ratio of straw to plastic is 1:1 in this article.

#### Effect of reaction temperature and Ni loading

Figures 4 and 5 show the effects of reaction temperature (ranging from 500 to 800 °C) and nickel load (from 5 wt.% to 20 wt.%) on gas concentration and H<sub>2</sub> production.

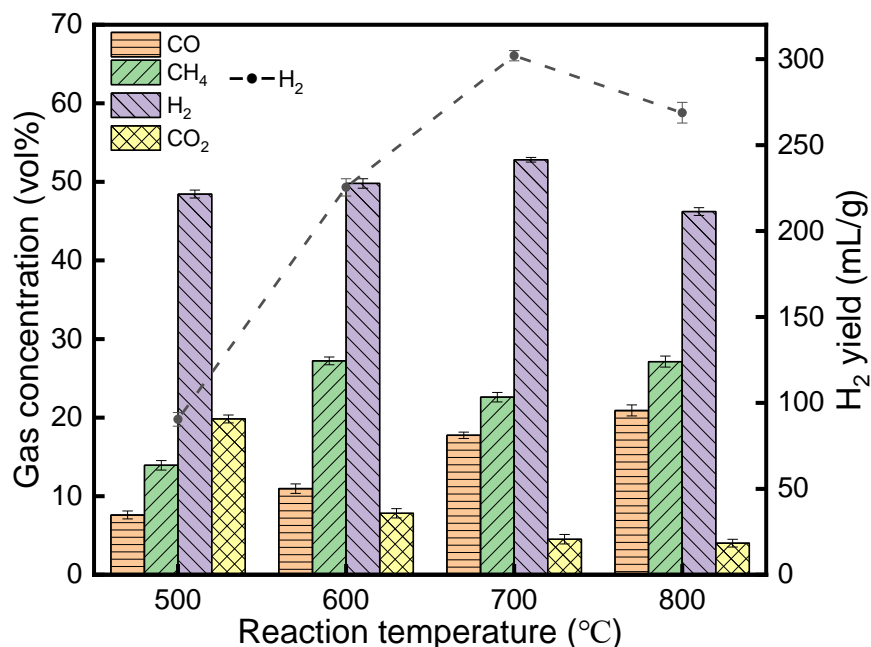


**Fig. 4.** Effect of reaction temperature on gas

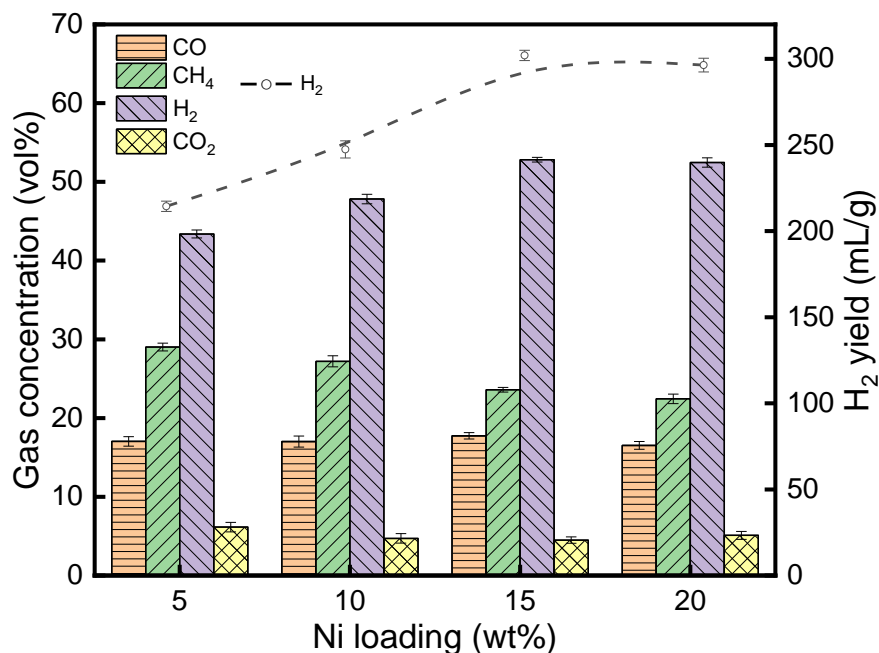


**Fig. 5.** Effect of Ni loading on gas

During this test, the calcination temperature and holding time were fixed at 400 °C and 20 min, respectively. The gas concentration and H<sub>2</sub> yield via mixtures pyrolysis were different as the reaction temperature and the total amount of nickel loaded were changed.

As shown in Fig. 4, with the temperature ranging from 500 to 800 °C, the H<sub>2</sub> concentration and yield first increased and then decreased, and reached the maximum at 700 °C, at 52.8 vol% and 302 mL/g, respectively. At the same time, the concentration of CH<sub>4</sub> was the lowest at 500 °C, But at this time, the yield of H<sub>2</sub> was very low compared to 700 °C, and among 600, 700, and 800 °C, the CH<sub>4</sub> concentration was lowest at 700 °C. Meanwhile, the concentration of CO increased with the increase of temperature. Therefore, a pyrolysis temperature of 700 °C was selected.

Figure 5 shows that as the nickel load increased, when the reaction temperature was 700 °C, the H<sub>2</sub> concentration and yield gradually increased, but when the load increased from 15 wt% to 20 wt%, there was little change in the concentration and yield, so a nickel load of 15 wt% was chosen.

#### *Effect of the holding time*

The effect of the holding time (ranging from 5 min to 30 min) on the gas concentration was studied with a total Ni loading amount of 15 wt.%, a reaction temperature of 700 °C, and a calcination temperature of 400 °C. The dependence of the H<sub>2</sub>, CO, and CH<sub>4</sub> concentration on the holding time is depicted in Fig. 6 (a), (b), and (c), respectively. As the holding time increased, the H<sub>2</sub> and CO concentrations also increased, but when the holding time exceeded 20 min, the concentration continued to only slightly increase. Similarly, the change of CH<sub>4</sub> concentration was the opposite; therefore, a holding time of 20 min was chosen. Compared with no catalyst at the same time, with the addition of the Ni/HC catalyst, the H<sub>2</sub> and CO concentrations increased from 20.6 vol.% and 10.8 vol.% to 52.8 vol% and 17.8 vol%, respectively. Meanwhile, the CH<sub>4</sub> concentration decreased from 51.1 vol% to 22.6 vol%.



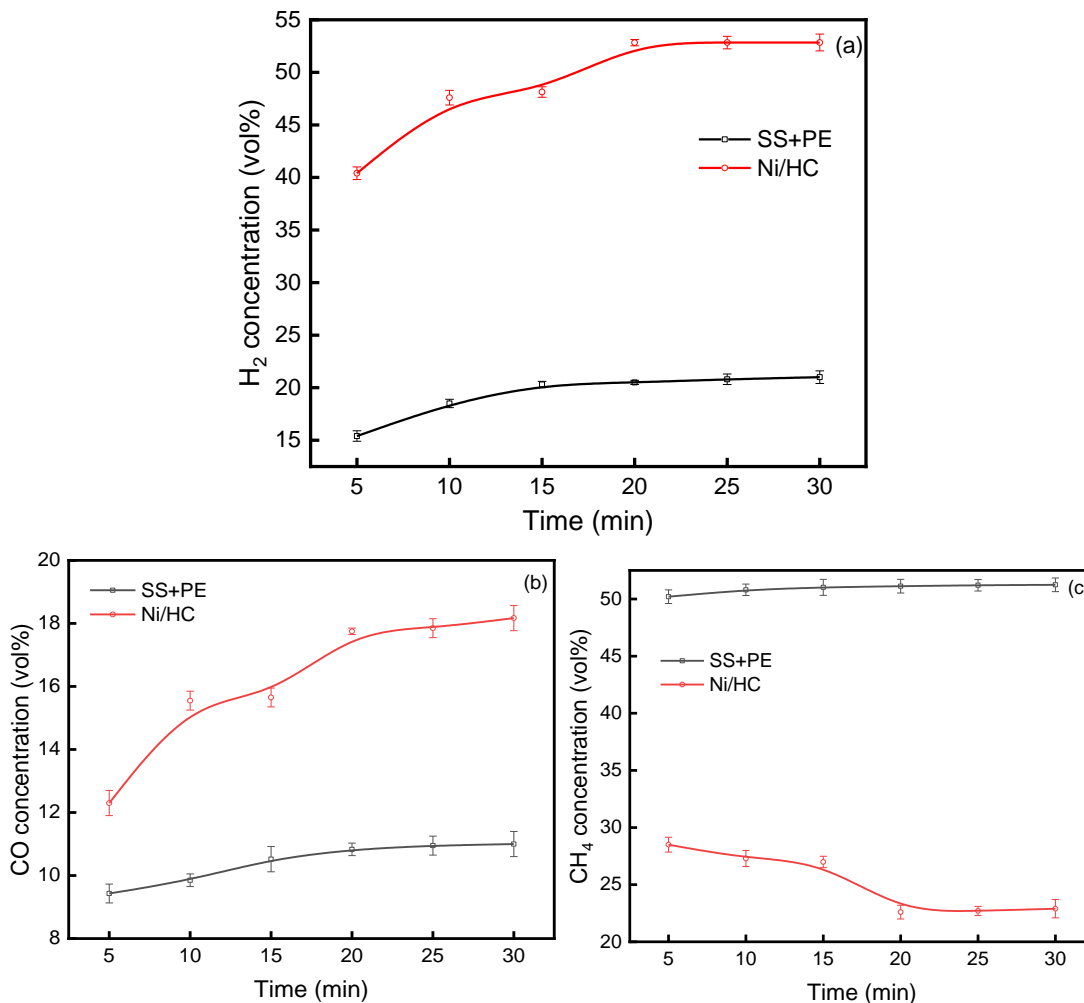


Fig. 6. Effect of the holding time on the syngas concentration: (a) H<sub>2</sub>, (b) CO, (c) CH<sub>4</sub>

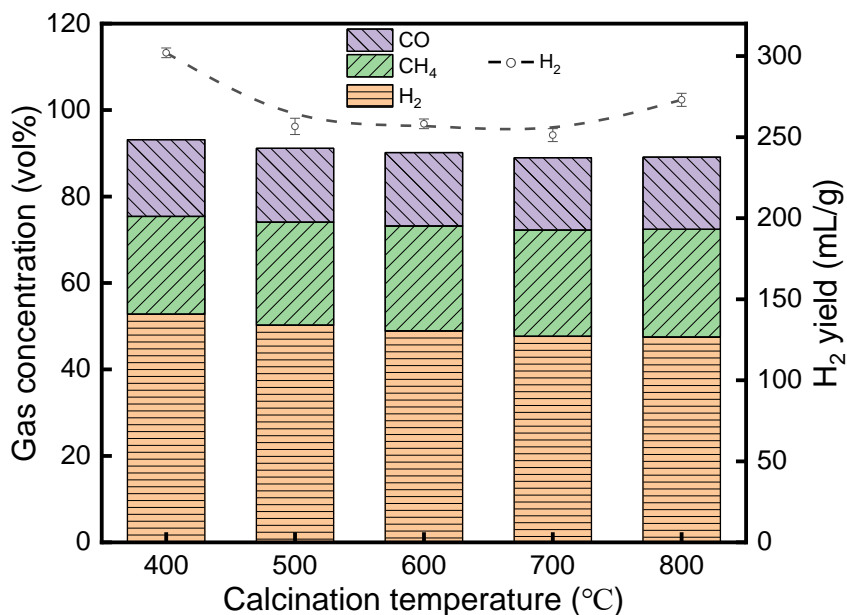


Fig. 7. Effect of the calcination temperature on the gas concentration

### Effect of the calcination temperature

The effects of calcination temperature (ranging from 400 and 800 °C) on the gas concentration was studied with a nickel loading, reaction temperature, and holding time of 15 wt.%, 700 °C, and 20 min, respectively. Figure 7 shows the change in gas concentration as the calcination temperature of the catalyst was increased. At a calcination temperature of 400 °C, the concentration and yield of H<sub>2</sub> reached its peak value of 52.8 vol% and 302 mL/g, respectively. The concentration of combustible gas (H<sub>2</sub>, CO, and CH<sub>4</sub>) was 93.2 vol%. As the calcination temperature was increased from 400 °C to 800 °C, the gas concentration decreased. Therefore, the optimum calcination temperature was 400 °C.

### Regeneration of the used catalyst

Recycling and reuse of the used catalyst in the catalytic pyrolysis process were investigated by an oxidative thermal treatment. The used catalyst was heated from 20 to 700 °C with a rate of 10 °C /min in an air atmosphere and maintained at 700 °C for 2 h. The thermal stability of filamentous carbon in catalyst carbon deposition is between 550 and 700 °C (Acomb *et al.* 2015; Yao *et al.* 2018; Yao and Wang 2020), so 700 °C was selected to regenerate the catalyst.

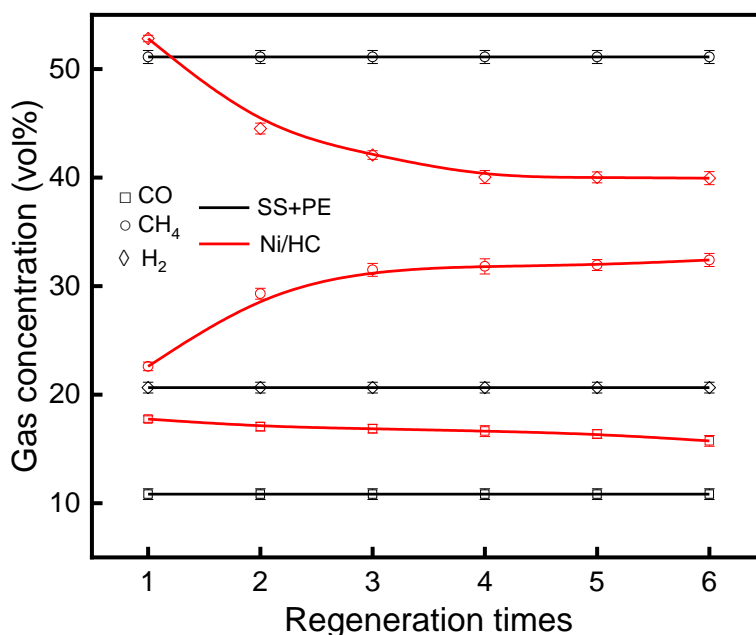


Fig. 8. Effect of catalyst regeneration times

Figure 8 shows that with the increase in regeneration times of the catalyst, the concentration of H<sub>2</sub> and CO gradually decreased, and the concentration of CH<sub>4</sub> increased gradually. However, compared with the case without the catalyst, the H<sub>2</sub> concentration was still approximately 40 vol%, and the total combustible gas concentration was approximately 80 vol%, which indicates that Ni/HC catalyst still had good catalytic activity after regeneration.

## CONCLUSIONS

1. Honeycomb cinder (HC) as catalyst carrier not only can solve problems of the rural environment, but it also has good catalytic activity as catalyst carrier, which can improve the concentration and yield of H<sub>2</sub> in co-pyrolysis gas of straw and plastic. It can provide some reference for the waste utilization in rural areas. After that, the catalyst can be modified by adding additives to investigate its catalytic activity.
2. The active component nickel was successfully loaded on the surface of honeycomb cinder (HC) in the form of NiO by homogeneous precipitation, and the NiO was evenly dispersed.
3. The optimum performance of the Ni/HC catalyst for the production of combustible gas was obtained at a calcination temperature of 400 °C, reaction temperature of 700 °C, holding time of 20 min, and Ni loading of 15 wt%.
4. When the reaction temperature was increased from 500 to 800 °C, the concentration and yield of H<sub>2</sub> first increased and then decreased, and reached the peak at 700 °C.
5. With the Ni/HC catalyst, the H<sub>2</sub> concentration increased from 20.6 vol% to 52.8 vol% and the highest hydrogen yield was 302 mL/g. The CH<sub>4</sub> concentration decreased from 51.1 vol% to 22.6 vol%.
6. The Ni/HC catalyst still had a certain catalytic activity after 6 times of regeneration, and the H<sub>2</sub> concentration was maintained at approximately 40 vol%

## ACKNOWLEDGMENTS

The authors are grateful for the support of the building project of Hubei Province for technology innovation and entrepreneurship service capacity Grant No. 2018BEC466, and the Central Committee Guides Local Science and Technology Development Special Project of Hubei Province, Grant No. 2018ZYYD062.

## REFERENCES CITED

- Acomb, J. C., Wu, C., and Williams, P. T. (2015). "Effect of growth temperature and feedstock:catalyst ratio on the production of carbon nanotubes and hydrogen from the pyrolysis of waste plastics," *Journal of Analytical and Applied Pyrolysis* 113, 231-238. DOI: 10.1016/j.jaap.2015.01.012
- Ahrenfeldt, J., Egsgaard, H., Stelte, W., Thomsen, T., and Henriksen, U. B. (2013). "The influence of partial oxidation mechanisms on tar destruction in TwoStage biomass gasification," *Fuel* 112, 662-680. DOI: 10.1016/j.fuel.2012.09.048
- Alvarez, J., Kumagai, S., Wu, C., Yoshioka, T., Bilbao, J., Olazar, M., and Williams, P. T. (2014). "Hydrogen production from biomass and plastic mixtures by pyrolysis-gasification," *International Journal of Hydrogen Energy* 39(21), 10883-10891. DOI: 10.1016/j.ijhydene.2014.04.189
- Anis, S., and Zainal, Z. A. (2011). "Tar reduction in biomass producer gas via mechanical, catalytic and thermal methods: A review," *Renewable and Sustainable Energy Reviews* 15(5), 2355-2377. DOI: 10.1016/j.rser.2011.02.018

- Block, C., Ephraim, A., Weiss-Hortala, E., Minh, D. P., Nzihou, A., and Vandecasteele, C. (2018). "Co-pyrogasification of plastics and biomass, A review," *Waste and Biomass Valorization* 10(3), 483-509. DOI: 10.1007/s12649-018-0219-8
- Burra, K. G., and Gupta, A. K. (2018). "Synergistic effects in steam gasification of combined biomass and plastic waste mixtures," *Applied Energy* 211, 230-236. DOI: 10.1016/j.apenergy.2017.10.130
- Cao, Y., Fu, L., and Mofrad, A. (2019). "Combined-gasification of biomass and municipal solid waste in a fluidized bed gasifier," *Journal of the Energy Institute* 92(6), 1683-1688. DOI: 10.1016/j.joei.2019.01.006
- Chai, Y., Gao, N., Wang, M., and Wu, C. (2020). "H<sub>2</sub> production from co-pyrolysis/gasification of waste plastics and biomass under novel catalyst Ni-CaO-C," *Chemical Engineering Journal* 382. DOI: 10.1016/j.cej.2019.122947
- Charisiou, N. D., Papageridis, K. N., Siakavelas, G., Tzounis, L., Kousi, K., Baker, M. A., Hinder, S. J., Sebastian, V., Polychronopoulou, K., and Goula, M. A. (2017). "Glycerol steam reforming for hydrogen production over nickel supported on alumina, zirconia and silica catalysts," *Topics in Catalysis* 60(15-16), 1226-1250. DOI: 10.1007/s11244-017-0796-y
- Chen, M., Li, X., Wang, Y., Wang, C., Liang, T., Zhang, H., Zhonglian, Y., Zhongshan, Z., and Wang, J. (2019). "Hydrogen generation by steam reforming of tar model compounds using lanthanum modified Ni/sepiolite catalysts," *Energy Conversion and Management* 184, 315-326. DOI: 10.1016/j.enconman.2019.01.066
- Chen, S., Meng, A., Long, Y., Zhou, H., Li, Q., and Zhang, Y. (2015). "TGA pyrolysis and gasification of combustible municipal solid waste," *Journal of the Energy Institute* 88(3), 332-343. DOI: 10.1016/j.joei.2014.07.007
- Déparrois, N., Singh, P., Burra, K. G., and Gupta, A. K. (2019). "Syngas production from co-pyrolysis and co-gasification of polystyrene and paper with CO<sub>2</sub>," *Applied Energy* 246, 1-10. DOI: 10.1016/j.apenergy.2019.04.013
- Fahmy, T. Y. A., Fahmy, Y., Mobarak, F., El-Sakhawy, M., and Abou-Zeid, R. E. (2018). "Biomass pyrolysis: Past, present, and future," *Environment, Development and Sustainability* 22(1), 17-32. DOI: 10.1007/s10668-018-0200-5
- Ghorbannezhad, P., Park, S., and Onwudili, J. A. (2020). "Co-pyrolysis of biomass and plastic waste over zeolite- and sodium-based catalysts for enhanced yields of hydrocarbon products," *Waste Manag* 102, 909-918. DOI: 10.1016/j.wasman.2019.12.006
- Grams, J., and Ruppert, A. (2017). "Development of heterogeneous catalysts for thermochemical conversion of lignocellulosic biomass," *Energies* 10(4). DOI: 10.3390/en10040545
- Levine, S. E., and Broadbent, L. J. (2009). "Detailed mechanistic modeling of high-density polyethylene pyrolysis: Low molecular weight product evolution," *Polymer Degradation and Stability* 94(5), 810-822. DOI: 10.1016/j.polymdegradstab.2009.01.031
- Lopez, G., Erkiaga, A., Amutio, M., Bilbao, J., and Olazar, M. (2015). "Effect of polyethylene co-feeding in the steam gasification of biomass in a conical spouted bed reactor," *Fuel* 153, 393-401. DOI: 10.1016/j.fuel.2015.03.006
- Moghadam, R. A., Yusup, S., Uemura, Y., Chin, B. L. F., Lam, H. L., and Al Shoaibi, A. (2014). "Syngas production from palm kernel shell and polyethylene waste blend in fluidized bed catalytic steam co-gasification process," *Energy* 75, 40-44. DOI: 10.1016/j.energy.2014.04.062

- Saxena, R. C., Adhikari, D. K., and Goyal, H. B. (2009). "Biomass-based energy fuel through biochemical routes: A review," *Renewable and Sustainable Energy Reviews* 13(1), 167-178. DOI: 10.1016/j.rser.2007.07.011
- Wang, S., Dai, G., Yang, H., and Luo, Z. (2017). "Lignocellulosic biomass pyrolysis mechanism: A state-of-the-art review," *Progress in Energy and Combustion Science* 62, 33-86. DOI: 10.1016/j.pecs.2017.05.004
- Xu, D., Xiong, Y., Ye, J., Su, Y., Dong, Q., and Zhang, S. (2020). "Performances of syngas production and deposited coke regulation during co-gasification of biomass and plastic wastes over Ni/ $\gamma$ -Al<sub>2</sub>O<sub>3</sub> catalyst: Role of biomass to plastic ratio in feedstock," *Chemical Engineering Journal* 392. DOI: 10.1016/j.cej.2019.123728
- Yao, D., and Wang, C. H. (2020). "Pyrolysis and in-line catalytic decomposition of polypropylene to carbon nanomaterials and hydrogen over Fe- and Ni-based catalysts," *Applied Energy* 265. DOI: 10.1016/j.apenergy.2020.114819
- Yao, D., Wu, C., Yang, H., Zhang, Y., Nahil, M. A., Chen, Y., Williams, P. T., Chen, H. (2017). "Co-production of hydrogen and carbon nanotubes from catalytic pyrolysis of waste plastics on Ni-Fe bimetallic catalyst," *Energy Conversion and Management* 148, 692-700. DOI: 10.1016/j.enconman.2017.06.012
- Yao, D., Yang, H., Chen, H., and Williams, P. T. (2018). "Investigation of nickel-impregnated zeolite catalysts for hydrogen/syngas production from the catalytic reforming of waste polyethylene," *Applied Catalysis B: Environmental* 227, 477-487. DOI: 10.1016/j.apcatb.2018.01.050
- Zhang, H., Nie, J., Xiao, R., Jin, B., Dong, C., and Xiao, G. (2014). "Catalytic co-pyrolysis of biomass and different plastics (polyethylene, polypropylene, and polystyrene) to improve hydrocarbon yield in a fluidized-bed reactor," *Energy and Fuels* 28(3), 1940-1947. DOI: 10.1021/ef4019299
- Zhang, X., Lei, H., Zhu, L., Qian, M., Zhu, X., Wu, J., and Chen, S. (2016). "Enhancement of jet fuel range alkanes from co-feeding of lignocellulosic biomass with plastics via tandem catalytic conversions," *Applied Energy* 173, 418-430. DOI: 10.1016/j.apenergy.2016.04.071
- Zhang, Z., Liu, L., Shen, B., and Wu, C. (2018). "Preparation, modification and development of Ni-based catalysts for catalytic reforming of tar produced from biomass gasification," *Renewable and Sustainable Energy Reviews* 94, 1086-1109. DOI: 10.1016/j.rser.2018.07.010
- Zhou, H., Meng, A., Long, Y., Li, Q., and Zhang, Y. (2014). "Classification and comparison of municipal solid waste based on thermochemical characteristics," *J Air Waste Manag Assoc* 64(5), 597-616. DOI: 10.1080/10962247.2013.873094

Article submitted: September 4, 2020; Peer review completed: November 7, 2020; Revised version received and accepted: November 9, 2020; Published: November 13, 2020.  
DOI: 10.15376/biores.16.1.223-235